Mechanisms regulating the large-scale seasonal fluctuations in *Alexandrium fundyense* populations in the Gulf of Maine: results from a physical-biological model

D.J. McGillicuddy, Jr.[1], D.M. Anderson[1]
D.R. Lynch[2], and D.W. Townsend[3]

Manuscript revised and resubmitted to Deep-Sea Research II
Ecology and Oceanography of Harmful Algal Blooms in the Gulf of Maine

April 27, 2005

[1] Woods Hole Oceanographic Institution, Woods Hole, MA 02543, USA. Tel: 508-289-2683 Fax: 508-457-2194 Email: dmcgillicuddy@whoi.edu (Corresponding Author).
[2] Thayer School of Engineering, Dartmouth College, Hanover, NH 03755, USA.
[3] School of Marine Sciences, University of Maine, Orono, ME 04469, USA.

Abstract

Observations of *Alexandrium fundyense* in the Gulf of Maine indicate several salient characteristics of the vegetative cell distributions: patterns of abundance are gulf-wide in geographic scope; their main features occur in association with the Maine Coastal Current; and the center of mass of the distribution shifts upstream from west to east during the growing season from April to August. The mechanisms underlying these aspects are investigated using coupled physical-biological simulations that represent the population dynamics of *A. fundyense* within the seasonal mean flow. A model that includes germination, growth, mortality, and nutrient limitation is qualitatively consistent with the observations. Germination from resting cysts appears to be a key aspect of the population dynamics that confines the cell distribution near the coastal margin, as simulations based on a uniform initial inoculum of vegetative cells across the Gulf of Maine produces blooms that are broader in geographic extent than is observed. In general, cells germinated from the major cyst beds (in the Bay of Fundy and near Penobscot and Casco Bays) are advected in the alongshore direction from east to west in the coastal current. Growth of the vegetative cells is limited primarily by temperature from April through June throughout the gulf, whereas nutrient limitation occurs in July and August in the western gulf. Thus the seasonal shift in the center of mass of cells from west to east can be explained by changing growth conditions: growth is more rapid in the western gulf early in the season due to warmer temperatures, whereas growth is more rapid in the eastern gulf later in the season due to severe nutrient limitation in the western gulf during that time period. A simple model of encystment based on nutrient limitation predicts deposition of new cysts in the vicinity of the observed cyst bed offshore of Casco and Penobscot Bays, suggesting a pathway of re-seeding the bed from cells advected downstream in the coastal current. A retentive gyre at the mouth of the Bay of Fundy tends to favor re-seeding that cyst bed from local populations.

Key words: phytoplankton, population dynamics, red tides, paralytic shellfish poisoning, USA, Gulf of Maine.

Introduction

The meroplanktonic dinoflagellate *Alexandrium fundyense* is subject to a wealth of physical-biological interactions that influence its distribution and variability (Anderson, 1998; Eilertsen and Wyatt, 2000; Wyatt and Jenkinson, 1997; Yamamoto et al., 2002). Its life cycle includes both a resting cyst and a planktonic phase of vegetative growth, giving rise to three basic linkages between its population dynamics and the physical environment. First, vital rates of *A. fundyense*'s population dynamics processes (excystment, vegetative growth, encystment) are influenced by ambient conditions including temperature, salinity, light, and nutrients. Second, the spatial distributions of the planktonic populations are constantly redistributed by ocean currents. Third, the organism is capable of directed motion through the water by virtue of its swimming ability. This tripartite linkage poses challenges to understanding the processes that control *A. fundyense* blooms: differentiation between the three sources of variability requires accurate assessment of the physical, biological, and chemical environment in space and time, in addition to detailed knowledge of the organism's behavioral capabilities and the processes by which ambient conditions control its vital rates. Herein we attempt to diagnose these multiple interactions using a coupled physical-biological model together with observations from the Gulf of Maine.

Anderson (1997) reviewed bloom dynamics of *A. fundyense*[1] in the northeast United States. The presence of the organism in coastal waters is manifested by the occurrence of paralytic shellfish poisoning (PSP) toxicity, which results from saxitoxins produced by *A.*

[1] Both *A. tamarense* and *A. fundyense* occur in the Gulf of Maine (Anderson et al., 1994). We consider these to be varieties of the same species (Anderson et al. 1994; Scholin et al. 1995). Neither antibody nor oligonucleotide probes can distinguish between them, and only detailed analysis of the thecal plates on individual cells can provide this resolution. This is not practical for large numbers of field samples. Accordingly, for the purpose of this study, the name *A. fundyense* is used to refer to both forms.

fundyense that accumulate in the tissues of filter feeding bivalves such as mussels and clams. Patterns of PSP toxicity indicate widespread occurrence in the Gulf of Maine, although the distribution is far from uniform. For example, the Penobscot Bay region (see Figure 1 for geographic references) is generally devoid of PSP, despite being flanked to the east and west by regions of high toxicity (Shumway et al., 1988). PSP tends to be less severe in western Maine and Massachusetts, with peak toxicity occurring early in the bloom season (May-June). Further to the east, in eastern Maine and the Bay of Fundy, peak toxicities can be nearly an order of magnitude higher than in the west, and occur toward the end of the bloom season (July-August). These regional differences in the timing and severity of PSP bespeak complex structure in the regional oceanography of *A. fundyense*.

Various aspects of *A. fundyense* bloom ecology have been studied in regional subdomains of the Gulf of Maine. Martin and White (1988) documented abundant vegetative cells at the mouth of the Bay of Fundy whose distribution generally overlaps with high concentrations of resting cysts in the underlying sediments (White and Lewis, 1982). Several findings of these studies are indicative of a self-sustaining population: (1) all of the various life cycle stages (cysts, vegetative cells, gametes, swimming zygotes [planozygotes]) are found in the same area, (2) fewer, if any, vegetative cells were found in upstream source waters inside the Bay of Fundy or on the Scotian Shelf, and (3) retentive characteristics of the local hydrodynamic environment, with a cyclonic gyre located at the mouth of the Bay of Fundy. That the Bay of Fundy population could be self-sustaining does not preclude a significant efflux of organisms into the Maine Coastal Current. Indeed, several of the surveys conducted by Martin and White (1988) are indicative of westward penetration of high cell densities into the Gulf of Maine.

A. fundyense blooms have been studied in the western Gulf of Maine as well. Anderson and Keafer (1985) noted the presence of high concentrations of cysts ca. 30 km northeast of Cape Ann, although the spatial extent of the deposit was not delineated fully. Hydrographic survey data revealed cell populations in the coastal waters with peak concentrations on the order of hundreds to thousands of cells per liter, generally associated with plumes of fresh water emanating from riverine sources (Franks and Anderson, 1992a). In fact, the north-to-south progression of toxicity within the western Gulf of Maine (south of Penobscot Bay) can be explained by alongshore transport of cells in coastally-trapped river plumes (Franks and Anderson, 1992b).

The nature of the interconnections between regional bloom phenomena within the Gulf of Maine remained enigmatic until the first coordinated gulf-wide study was carried out during 1997-2001 in the Ecology and Oceanography of Harmful Algal Blooms – Gulf of Maine (ECOHAB-GOM) program. A systematic cyst survey (Anderson et al., submitted) revealed that the western Gulf of Maine cyst deposit originally discovered by Anderson and Keafer (1985) was much larger than previously thought, broadly distributed in the offshore waters from Casco Bay to Penobscot Bay (Figure 2a). Vegetative cell distributions were found to be gulf-wide in character (Figure 3; also see Townsend et al. 2001)[2]. Peak cell concentrations occur in association with the Maine Coastal Current. Moreover, the center of mass shifts from west to east (progressively upstream with respect to the coastal current) as the season progresses from June to August. Also evident is the persistence of high cell abundance at the mouth of the Bay of Fundy, geographically associated with a large peak in the distribution of benthic cysts (Figure

[2] Note that the Townsend et al. (2001) cell counts were based on an antibody probe that does not distinguish between *A. fundyense* and *A. ostenfeldii*. The former produces saxitoxins, whereas the latter does not. These two species co-occur in the Gulf of Maine (Gribble et al., submitted), such that their relative concentrations can fluctuate significantly.

2a). Although the observations presented in Figure 3 come from only a single year (1998), subsequent surveys by the ECOHAB-GOM program in 2000 and 2001 generally corroborate these findings (Townsend et al., submitted-b). Relative stability of the gulf-wide mean abundance of vegetative cells on interannual time scales (McGillicuddy et al., submitted) further attests to the fact that there is a climatology of *A. fundyense* to be explained.

Our goal herein is to elucidate the mechanisms responsible for four prominent aspects of the large-scale seasonal variations in *A. fundyense* populations in the Gulf of Maine: (1) the vegetative cell distributions are gulf-wide in character; (2) peak cell concentrations occur in association with the Maine Coastal Current; (3) the center of mass of the cell distribution shifts from west to east as the growing season progresses; and (4) benthic cyst beds persist at the mouth of the Bay of Fundy and offshore of Casco and Penobscot Bays. The approach is to incorporate a model of *A. fundyense* population dynamics developed for the western Gulf of Maine (Stock et al., submitted) into a model of the seasonal mean circulation in the region (Lynch et al., 1996). In so doing we seek to understand the degree to which the observations can be explained by the organism's population dynamics together with the mean circulation. By no means does this discount the potential importance of higher frequency and smaller scale phenomena in regulating blooms of *A. fundyense* in the Gulf of Maine. Indeed, synoptic-scale variability appears to play a role not only in regional bloom dynamics (Franks and Anderson, 1992ab; Keafer and Anderson, 1993; Anderson et al., 2005; Keafer et al., submitted; Luerssen et al., submitted), but also in determining mean properties of the system such as the cross-isobath transport of cells (Hetland et al., 2002; McGillicuddy et al., 2003). However, given the prominent aspects of the mean circulation in the Gulf of Maine (Bigelow, 1927), superposition of

the mean physics with the mean biology constitutes a logical starting point for investigating the large-scale seasonal bloom dynamics.

The experimental design (Table 1) consists of four simulations, aimed at isolating the key population dynamics processes. The space/time distribution of vegetative cells in the coastal current due to germination of resting cysts is first quantified (Run 1). The effects of growth and mortality are then added (Run 2). Next a nutrient limitation term is included in the model (Run 3), resulting in a simulation that matches the three main characteristics of the observations listed above. Lastly, the most realistic case (Run 3) is rerun with a uniform initial inoculum of vegetative cells instead of the germination-based source of cells. Comparison of this final case (Run 4) with its predecessor provides information about the role of cyst germination in shaping the characteristics of the simulated blooms.

Methods

Circulation model

The hydrodynamic basis for this study is a finite element circulation model of the Gulf of Maine / Georges Bank region described in Lynch et al. (1996). The finite element methodology facilitates realistic representation of the complex geometry in this area. Horizontal grid spacing in regions of steep topography is as fine as 1 km, and coarser where such high resolution is not required. The three-dimensional model is hydrostatic, non-linear, and incorporates advanced turbulence closure. Published solutions for the climatological mean circulation, broken down into six bi-monthly periods, are demonstrably consistent with available observations (Naimie, 1996; Naimie et al., 2001).

Lynch et al. (1997) describe simulations of the climatological springtime circulation in the Maine Coastal Current (MCC) system, which are particularly relevant to the present context. The conceptual model underlying these simulations consists of a set of interconnected segments with several branch points (Figure 1). The eastern segment of the MCC extends from the mouth of the Bay of Fundy to Penobscot Bay, where an offshore meander occurs (Brooks, 1985). At this point the current branches into two segments, one that continues along the coast and another that veers offshore around the Jordan Basin Gyre. Potential mechanisms affecting the path of this offshore branch include topographic effects, offshore steering along the southwestern flank of the cyclonic gyre over Jordan Basin (Bisagni et al., 1996; Brooks and Townsend, 1989), and inshore influences of the Penobscot river plume that tend to push the current offshore (Brooks, 1994; Pettigrew et al., 1998; Xue et al., 2000). The Western segment of the MCC is fed by the inshore branch of the eastern segment together with the outflow of the Penobscot River. The western segment accumulates local contributions from the Kennebec, Androscoggin, Saco, and Merrimack Rivers in its southwestward transit toward a second branch point offshore of Cape Ann. At this point, a portion of the flow turns inshore into Massachusetts and Cape Cod Bays, then rejoining the current north and east of Cape Cod (Blumberg et al., 1993; Signell et al., 1993). Further downstream, the current undergoes yet another bifurcation, with one branch flowing toward Nantucket Shoals, and another feeding the clockwise circulation around Georges Bank. Each of these basic features of the flow are represented within the circulation model on which this study is based.

Archived solutions of the hydrodynamic model are stored in a form that is available for use in an off-line transport code “Acadia” which solves a depth-integrated form of the advection-diffusion-reaction equation on the same grid using the archived hydrodynamic information as

input. Within this framework, the coupled physical-biological model for vertically averaged plankton concentration C is written

$$\frac{\partial C}{\partial t} + v \cdot \nabla C - \frac{1}{H} \nabla (HK \nabla C) = R$$

where v is the velocity, K the diffusivity, H the bottom depth, and R the biological "reaction" term that represents *A. fundyense* population dynamics (including excystment, growth, and removal processes). Vertically averaged climatological mean velocity and diffusivity fields are specified from the bi-monthly archive. Boundary conditions consist of (1) no flux through solid boundaries (excepting that which occurs via excystment), (2) specification of concentration at inflow, or (3) computation of concentration at outflow assuming no diffusive flux (i.e. $K \nabla C \cdot \hat{n} = 0$).

This vertically averaged hydrodynamic framework precludes explicit representation of vertical structure in *A. fundyense* populations in the water column. As such, the effects of *A. fundyense*'s swimming ability are parameterized in a very basic manner. That is, newly germinated cells are assumed to reach surface waters instantly, in contrast to the multiple days it would actually take to reach the surface swimming upwards at 10 m d^{-1} from deep offshore cyst beds. This effectively eliminates the downstream advection of cells that would take place during their transit upward. A potentially more serious shortcoming of this simple formulation is the lack of vertical migration behavior that could allow *A. fundyense* to exploit nutrients present in subsurface layers (MacIntyre et al., 1997). However, recent evidence suggests that the capability for vertical migration is not universal amongst all strains of *A. fundyense* from the Gulf of Maine (Poulton, 2001). Moreover, the importance of this behavior has yet to be demonstrated unequivocally in natural populations of *A. fundyense* in the gulf (Martin et al.,

submitted; Townsend et al., submitted-a). Because of this uncertainty about the importance of vertical migration, we have chosen not to include it in these simulations.

Population dynamics model

Fundamental to this modeling approach is the concept that the ecosystem in which *A. fundyense* resides is not explicitly modeled. This is justified on the basis that, with few exceptions, *A. fundyense* constitutes a very small fraction of the phytoplankton species assemblage in the Gulf of Maine. As such, it generally does not significantly influence either the ambient nutrient fields or predator distributions. Therefore, ecosystem effects are parameterized through their influence on the vital rates of *A. fundyense*'s population dynamics processes.

The *A. fundyense* population dynamics model used in this study is summarized in Figure 2. Model parameters and their definitions are presented in Table 2. Parameter choices were guided by application of the same biological formulation in a three-dimensional model of the western Gulf of Maine, in which optimal parameters were deduced from a Maximum Likelihood fit to observations in that region (Stock et al., submitted). Because the population dynamics model has been "tuned" to the region (albeit with a data set that covers only a subregion of the present domain), parameter optimization was not attempted in the present study. Note that there are minor differences between the parameter values used herein and the final values reported in Stock et al. (submitted). These differences are attributed to refinements in the Stock et al. analysis that took place subsequent to the conclusion of the present study.

An important caveat to this implementation of the population dynamics model is that it does not explicitly represent variability in behavioral characteristics or vital rate parameters

known to exist among various strains of *A. fundyense* (c.f. discussion of vertical migration above). The traditional approach in modeling planktonic population dynamics is to formulate the model in terms of the mean biological properties, which are assumed to be representative of the population. If subpopulations exhibit significant differences in physiological and/or behavioral responses to environmental conditions, yet another source of spatiotemporal variability is introduced into the coupled physical-biological problem. In the present application, we assess the degree to which the gulf-wide seasonal evolution of *A. fundyense* can be modeled as a single population. Future work will investigate the issue of intraspecific variability in the organism's population dynamics (http://www.whoi.edu/science/cohh/whcohh/index.htm; see Research Projects 1 and 2).

The flux of vegetative cells into the water column is specified by the observed distribution of resting cysts (Figure 2a) together with *A. fundyense's* endogenous clock (*EC*, Figure 2b) and a germination rate (*G*) that depends on ambient temperature (*T*) and non-spectral irradiance (*E*) (Figure 2c). The flux of cells due to germination (F_g) is given by

$$\mathrm{F_g} = EC(t) \times G(T,E) \times d_g \times [Cysts/cm^3]_0$$

where the germination depth d_g is the vertical extent of the surficial sediment layer from which germinating cysts can gain the water column, and the cyst concentration $[Cysts/cm^3]_0$ is the initial cyst distribution specified from observations (Figure 2a).[3] This model assumes replenishment of the cyst beds on annual time scales, a process that can be fed by two different pathways: (1) formation and deposition of new cysts, and (2) sediment mixing. The latter mechanism arises from the fact that in this region, typical *A. fundyense* cyst profiles within the

[3] Cysts have also been observed suspended in the water column (Kirn et al., submitted). However, vertically integrated abundances of suspended cysts are generally at least an order of magnitude less than that present within the sediments. Therefore we do not include suspended cysts in the present model.

sediment contain a subsurface maximum located multiple centimeters below the oxygenated layer in which germination can occur (Keafer et al., 1992). Therefore mixing within the sediments due to bioturbation or other disturbances would tend to resupply the upper layer with cysts. For a detailed description of the cyst map, germination model, and cyst dynamics, see Anderson et al. (submitted). Matrai et al. (submitted) provide additional information on germination rates from cysts in the eastern Gulf of Maine.

Vegetative growth of *A. fundyense* depends on temperature and salinity. Temperature dependence *f(T)* is defined by a cubic polynomial fit to the laboratory data of Watras et al. (1982) and Anderson and Keafer (unpublished data):

$$f(T) = -0.000347T^3 + 0.0097T^2 - 0.0133T + 0.131 \qquad R^2 = 0.88$$

Salinity dependence *f(S)* is defined by a quadratic fit to the data of Watras et al. (1982) and Prakash (1967):

$$f(S) = -0.0022S^2 + 0.103S - 0.195 \qquad R^2 = 0.66$$

These functional fits agree qualitatively with the experimental determinations of growth rate reported in Etheridge and Roesler (submitted), which also suggest weak dependence on salinity and an optimal temperature range of approximately 10-15º C. Both *f(T)* and *f(S)* are scaled to vary between 0 and 1 to modulate the maximum growth rate ($\mu_{\max}$) for all *T* and *S* (Figure 2d):

$$\mu(T,S) = \mu_{\max} \times f(T) \times f(S)$$

Temperature and salinity fields are specified from the same climatology used to drive the hydrodynamic model (Figure 4, top two rows).

Dependence of vegetative growth on light and nutrients is modeled after Liebig's Law of the Minimum (Liebig, 1845):

$$\mu(E, NO_3, T, S) = \min\big(\mu(E,T,S), \mu(NO_3,T,S)\big)$$

Light-limited growth takes a hyperbolic form based on growth efficiency α_g and a basal respiration rate μ_0^r (Langdon, 1987; Langdon, 1988; Platt and Jassby, 1976):

$$\mu(E,T,S) = \left(\mu(T,S) + \mu_o^r\right)\tanh\left(\frac{\alpha_g E}{(\mu(T,S) + \mu_o^r)}\right) - \mu_o^r$$

where irradiance is averaged from the surface down to the 1% light depth using $E(z) = E_0 e^{-k_w z}$. Nutrient dependence is modeled by Michaelis-Menten kinetics with half-saturation constant K_N:

$$\mu(NO_3,T,S) = \mu(T,S) \times \frac{[NO_3]}{K_N + [NO_3]}$$

Nitrate fields are estimated from an empirical five-term polynomial fit between nitrate and temperature and salinity described in Garside et al. (1996). Because the Garside et al. fit does not accurately represent the high-nutrient low-salinity condition characteristic of river plume waters near the coast, nitrate concentrations in salinities less that 31.3 ppt were assigned values of the nearest neighboring point with salinity greater than 31.3 ppt. The resulting nitrate maps (Figure 4, third row) based on the climatological temperature and salinity fields are generally consistent with those reported in Petrie and Yeats (2000) in terms of their large-scale seasonal characteristics.

Losses of vegetative cells occur as a result of grazing by zooplankton as well as encystment. Both of these rates are difficult to quantify with measurements. Grazing losses inflicted on *A. fundyense* are a complex function of both the heterotrophic and autotrophic communities (Teegarden and Cembella, 1996; Turner and Tester, 1997; Campbell et al., submitted; Turner and Borkman, submitted). In the absence of observations sufficient to prescribe spatially and temporally varying grazing pressure on *A. fundyense*, we parameterize the impact of grazing with a constant specific loss rate *m* (day^{-1}).

Encystment results from a complex sequence of biological transformations that are initiated by sexual reproduction of vegetative cells. In laboratory cultures of *Alexandrium*, this process can be induced by nutrient stress in the form of nitrogen or phosphorus limitation (Anderson, 1998). However, the trigger for cyst formation in natural *A. fundyense* populations remains elusive (Anderson et al., 1984; Anderson and Lindquist, 1985; Turpin et al., 1978). Based on the laboratory studies, encystment was estimated from the modeled growth function, which is defined above as the lesser of the light- and nutrient-limited growth rates at ambient temperature and salinity conditions. When the nutrient limited growth rate is less than the light-limited growth rate, the specific rate of encystment (*En*) is proportional to their difference:

$$En = \frac{1}{2}\left(\mu(E,T,S) - \mu(NO_3,T,S)\right)C \qquad \mu(NO_3,T,S) < \mu(E,T,S)$$

$$En = 0 \qquad \mu(NO_3,T,S) \geq \mu(E,T,S)$$

In a sense, encystment is parameterized as that fraction of the vegetative cells that would have continued to grow were they not subject to nutrient limitation. The leading factor of ½ accounts for that fact that two vegetative cells fuse into a zygote that becomes a cyst. In this model, newly formed cysts are assumed to sink to the bottom instantly.

Results

The "germination only" case (Run 1) documents vegetative cell distributions resulting from the combined effects of hydrodynamic transport and spatial and temporal variations in excystment prescribed by the population dynamics model (Figure 5, left column). Early in the season, peaks in vegetative cell concentrations occur in association with epicenters of the cyst distribution located at the mouth of the Bay of Fundy and offshore of Casco and Penobscot Bays.

Under the influence of the coastal current system, newly germinated cells are advected downstream toward the south and west, such that by the end of the simulation a broad peak exists in the western Gulf of Maine. Traces of the cell population extend far to the south and east, where cells have been entrained into the clockwise circulation around Georges Bank. Low cell concentrations are evident all the way to the outflow boundary south of Cape Cod. Clearly, a great deal of spatiotemporal structure results simply from the input of cells into the complex circulation of this region. However, germination by itself is not sufficient to explain the seasonal increase in abundance of cells, as the simulated concentrations are considerably lower than is observed, particularly during the latter part of the season.

Inclusion of growth and mortality in the population dynamics model (Run 2) yields a vegetative cell population (Figure 5, middle column) that is considerably larger than the "germination only" case. Early in the growing season, the pattern is similar to the prior run but the concentrations are closer to those that are observed. Whereas May-June concentrations offshore of Casco Bay in the "germination only" case are generally less than 100 cells l^{-1}, concentrations in this area reach several hundred cells l^{-1} in the "germination and growth" simulation. Later in the season, simulated cell concentrations rapidly diverge from observations. By July, the model predicts thousands of cells l^{-1} in the western Gulf of Maine, where very few cells are observed that late in the growing season. High cell concentrations also arise in the near coastal waters south of Cape Cod, where *A. fundyense* is generally not found in high abundance. From July to August, the anomalously large cell concentrations in the western Gulf of Maine and south of Cape Cod continue to increase, further exacerbating the discrepancies between simulated and observed cell distributions in those areas.

The problematic late-season blooms in the western and southern portions of the domain are removed from the numerical solution by including nutrient limitation in the model (Run 3). Early in the simulation, prior to the onset of nutrient limitation, simulated cell concentrations (Figure 5, right column) are nearly identical to the prior run. From June through August, cell concentrations in the western Gulf of Maine and points south drop to near zero. Moreover, the center of mass in the cell distribution shifts from west to east as the growing season progresses. Whereas the peak abundance lies in a relatively small area offshore of Casco Bay in June, by August the peak is more broadly distributed and centered offshore of Penobscot Bay and further east.

It is worthy of note that the nutrient limited simulation predicts far lower concentrations of cells on Georges Bank. In the simulation without nutrient limitation (Figure 5, middle column), Georges Bank is inoculated by cells transported in from both the north and west. In contrast, the onset of nutrient limitation effectively closes the late-season transport pathway of cells east of Cape Cod, such that the only remaining delivery mechanism is southward transport from the Gulf of Maine interior (Figure 5, right column).

The large-scale seasonal fluctuations in *A. fundyense* predicted by the nutrient limited model (Run 3) are generally consistent with observations (Figure 3), yet some discrepancies still exist. For example, toward the latter part of the season, the simulated peaks in the cell distribution are broader and spread farther west than is observed. In addition, concentrations at the mouth of the Bay of Fundy are underestimated. Nevertheless, the simulation appears to capture the most general qualitative characteristics of the observed patterns.

When this same model for growth and mortality is used to drive a simulation based on a uniform initial inoculum of 10 cells l^{-1} everywhere in the domain (Run 4), model predictions

differ significantly from observations (Figure 6). The simulated population is much more oceanic than coastal in its overall character, with the center of mass much further offshore than is observed. Near-coastal waters are almost devoid of cells, except in the eastern Gulf of Maine later in the simulation.

Discussion

Of the four simulations presented herein, the run that includes germination, growth, mortality and nutrient limitation (Run 3) produces results that are most consistent with observations. It is therefore of interest to diagnose this run in more detail to understand the processes controlling the seasonal development of *A. fundyense* blooms in the model. Analysis of the various terms regulating growth rate is particularly useful in this regard (Figure 4). Generally speaking, the temperature/salinity component of the growth rate expression (fourth row) mimics the climatological temperature distribution; seasonal salinity variations have a relatively minor contribution to the gulf-wide patterns in growth rate. The nutrient limitation term (fifth row) contains significant seasonal variations with regional structure. Nitrate is in abundance in March-April, so the nutrient-limited growth rate is nearly identical to the temperature/salinity limited growth rate during that period. As the season progresses, nitrate concentration declines to levels that limit growth, particularly in the western gulf. Thus, the overall growth rate (sixth row) is primarily limited by temperature in March-April; by July-August, western gulf populations are severely nutrient limited, whereas population growth continues in the eastern gulf at the temperature-limited rate. Therefore, the upstream (eastward) shift in the center of mass of the simulated distribution can be explained by the onset of nutrient limitation in the western gulf, together with continued growth of the cell population in the east. This transition to nutrient

limitation in the western gulf is consistent with the findings of Love et al. (submitted), who document decreasing nitrate concentrations in the Casco Bay region during the period April to June. Poulton et al. (submitted) also suggest progressive nitrogen limitation of *A. fundyense* populations in that area on the basis of a seasonal trend in toxin composition.

In the model that produces these "best" case results, blooms of *A. fundyense* are initiated by germination from resting cysts, but vegetative growth plays a key role in regulating the large-scale seasonal patterns in abundance. It is relevant to inquire whether or not the cyst-driven source is a key aspect of the system. An alternative to the "cyst source" hypothesis is that vegetative growth controls the large-scale distribution of cells, such that the only source that is needed is a modest overwintering population. This hypothesis was tested by applying the very same growth and mortality model to a uniform initial inoculum of vegetative cells (Run 4). The results diverge significantly from the "best" case (Run 3). Whereas the model driven by germination results in coastal blooms with seasonal evolution that is generally consistent with observations, the model driven by a uniform initial inoculum produces offshore blooms with little in common with the observed distributions. This suggests that resting cysts play an important role in maintaining the coastal character of *A. fundyense* blooms in this region. However, it could be that the present model is missing some key aspect of *A. fundyense*'s growth response to environmental conditions—in particular growth stimulation in coastal waters and growth inhibition offshore. That seems unlikely, given that the growth kinetics of the genus *Alexandrium* are amongst the best studied of marine phytoplankton. Whatever factor that might be, it would have to impose severe cross-shelf gradients in the balance between growth and mortality of *A. fundyense*. For now the "cyst source" hypothesis appears to be the most compelling.

If the germination flux is a key bloom initiator, it is of considerable interest to determine whether or not climatological physical and biological conditions provide a conduit for maintaining the observed cyst distributions. Maps of the specific rate of encystment (Figure 4, bottom row) highlight the areas of nutrient limitation present in the growth function. There is negligible potential for encystment early in the season when nutrients are in abundance (March-April). Encystment begins in the extreme southwestern portion of the domain in May-June. By July-August, encystment potential is widespread in the western Gulf of Maine and in limited areas of the near-coastal environment of the eastern Gulf of Maine. Application of these specific rates to the vegetative cell population from the "best" simulation (Run 3) provides explicit predictions of cyst deposition (Figure 7). At the end of the simulation, there are two epicenters in the distribution of newly formed cysts: offshore of Casco and Penobscot Bays, and at the mouth of the Bay of Fundy. These locations generally coincide with the major peaks in the observed cyst distribution (Figure 2a), although the specific geographic details differ. One aspect of the predicted cyst deposition that is not consistent with observations is the relative magnitude of the peaks in the eastern and western Gulf of Maine. In the simulation, far fewer cysts are deposited at the mouth of the Bay of Fundy than in the western gulf, opposite to what would be expected based on the relative abundance of cysts. However, it is important to note that the growing season for *A. fundyense* in the eastern Gulf of Maine extends well into the fall (Page et al., 2002). Whether bloom termination in the east is controlled by nutrient limitation, an endogenous trigger in *A. fundyense*'s life cycle (Anderson, 1998), or some other factor is not known. Because of this uncertainty in the processes responsible for the autumn demise of the bloom in the eastern gulf, the present simulation ends in August and therefore the bulk of the cyst deposition in that area may not be accounted for. Nevertheless, these results suggest a

scenario for long-term maintenance of two distinct cyst beds in the Gulf of Maine: retention of a self-sustaining population in the Bay of Fundy gyre, together with downstream advection of that portion of the Bay of Fundy population that leaks out into the coastal current. In this model, the position of the downstream cyst bed is set by the length scale over which the transition to oligotrophy occurs as the Maine Coastal Current flows westward from the nutrient-rich waters of the eastern Gulf of Maine.

Conclusions

Results from the hierarchy of models presented herein provide a basis for distillation of a conceptual model for the large-scale seasonal dynamics of *A. fundyense* populations in the Gulf of Maine (Figure 8). Anderson et al. (submitted) describe a similar conceptual model that extends these dynamics further to the west. The growing season begins with synchronous germination from two major cyst beds located at the mouth of the Bay of Fundy and offshore of Casco and Penobscot Bays. Two factors favor higher vegetative cell concentrations in the western Gulf of Maine during spring: (1) higher growth rates due to warmer temperatures in that area, and (2) the cumulative impact of having been fed by both local and upstream (Bay of Fundy) cyst beds. With the transition from spring to summer comes the onset of nutrient depletion in the western Gulf of Maine, leading to cyst deposition at the terminus of high nutrient waters in the Maine Coastal Current. In the eastern Gulf of Maine, growth of vegetative cells continues due to the ample supply of nutrients still present in that area. Thus the seasonal west-to-east shift in the center of mass of vegetative cells occurs via a transition from temperature limitation of eastern populations in the spring and nutrient limitation of western populations in the summer. Counter-clockwise circulation in the gyre at the mouth of the Bay of Fundy tends to

retain cells in that area, leading to a late-summer peak in the cell distribution therein. The model suggests formation of new cysts in association with the late-summer Bay of Fundy population, although the bulk of the cyst deposition in this area may take place after the time period covered in these simulations.

Combination of the "mean physics" and the "mean biology" (expressed as a single population) produces results that are consistent with the general features of the observed large-scale variations in *A. fundyense* in the Gulf of Maine. A critical next step is to investigate perturbations about this mean state that underlie fluctuations on time scales ranging from synoptic to interannual. That activity will require data-assimilative hindcasts for specific time periods (He et al., submitted; Lynch and Hannah, 2001), together with quantitative methods for evaluating the fidelity of coupled physical-biological simulations (Stock et al., submitted).

Acknowledgments

We gratefully acknowledge the support of the U.S. ECOHAB Program, sponsored by NOAA, NSF, EPA, NASA, and ONR. We thank Charles Stock for providing the biological model code described in Stock et al. (submitted), and Dr. Valery Kosnyrev for implementing it into the climatological hydrodynamic framework. We thank Anita Norton and Sue Stasiowski for their assistance in preparing several figures. Constructive comments from two anonymous reviewers helped improve the original manuscript. This is WHOI contribution 11150, and ECOHAB contribution XXXX.

Correspondence and requests for materials to D.J. McGillicuddy, Jr. (dmcgillicuddy@whoi.edu).

References

Anderson, D.M., 1998. Physiology and Bloom Dynamics of Toxic *Alexandrium* Species, with emphasis on Life Cycle Transitions. In: D.M. Anderson, A.D. Cembella and G.M. Hallegraeff (Editors), Physiological Ecology of Harmful Algal Blooms. NATO ASI Series. Springer-Verlag, Berlin, pp. 29-48.

Anderson, D.M., Keafer, B.A., (Editors), 1985. Dinoflagellate cyst dynamics in coastal and estuarine waters. Toxic Dinoflagellates. Proceedings of the 3rd International Conference. Elsevier, New York.

Anderson, D.M., Keafer, B.A., 1987. An endogenous annual clock in the toxic marine dinoflagellate *Gonyaulax tamarensis*. Nature, 325: 616-617.

Anderson, D.M., Keafer, B.A., Geyer, W.R., Signell, R.P., Loder, T.C., 2005. Toxic *Alexandrium* blooms in the western Gulf of Maine: the "plume advection hypothesis" revisited. Limnology and Oceanography 50: 328-345.

Anderson, D.M., Kulis, D.M., Binder, B.J., 1984. Sexuality and cyst formation in the dinoflagellate *Gonyaulax tamarensis*: cyst yield in batch cultures. Journal of Phycology, 20: 418-425.

Anderson, D.M., Lindquist, N.L., 1985. Time-course measurements of phosphorous depletion and cyst formation in the dinoflagellate *Gonyaulax tamarensis* Lebour. Journal of Experimental Marine Biology and Ecology, 86(1): 1-13.

Anderson, D.M., Stock, C.A., Keafer, B.A., Bronzino, A., McGillicuddy, D.J., Keller, M.D., Thompson, B., Matrai, P.A., J. Martin, submitted. Experimental observations and modeling of *Alexandrium fundyense* cyst dynamics in the Gulf of Maine. Deep Sea Research II.

Bigelow, H.B., 1927. Physical oceanography of the Gulf of Maine. Bull. U.S. Bur. Fish., 40: 511-1027.

Bisagni, J.J., Gifford, D.J., Ruhsam, C.M., 1996. The spatial and temporal distribution of the Maine Coastal Current during 1982. Continental Shelf Research, 16(1): 1-24.

Blumberg, A.F., Signell, R.P., Jenter, H.L., 1993. Modelling transport processes in the coastal ocean. Journal of Marine Environmental Engineering, 1: 31-52.

Brooks, D.A., 1985. Vernal circulation in the Gulf of Maine. Journal of Geophysical Research, 90(C3): 4687-4705.

Brooks, D.A., 1994. A model study of the buoyancy-driven circulation in the Gulf of Maine. Journal of Physical Oceanography, 24: 2387-2412.

Brooks, D.A., Townsend, D.W., 1989. Variability of the coastal current and nutrient pathways in the eastern Gulf of Maine. Journal of Marine Research, 47: 303-321.

Campbell, R. G., Teegarden, G. J., Cembella, A. D., Durbin, E. G., submitted. Zooplankton grazing impacts on *Alexandrium* spp. in the nearshore environment of the Gulf of Maine. Deep Sea Research II.

Eilertsen, H.C., Wyatt, T., 2000. Phytoplankton models and life history strategies. South African Journal of Marine Science, 22: 323-338.

Etheridge, S. M., Roesler, C. S., submitted. Effects of temperature, irradiance, and salinity on photosynthesis, growth rates, total toxicity, and toxin composition for *Alexandrium fundyense* isolates from the Gulf of Maine and Bay of Fundy. Deep Sea Research II.

Franks, P.J.S., Anderson, D.M., 1992a. Alongshore transport of a phytoplankton bloom in a buoyancy current: *Alexandrium tamarense* in the Gulf of Maine. Marine Biology, 112: 153-164.

Franks, P.J.S., Anderson, D.M., 1992b. Toxic phytoplankton blooms in the southwestern Gulf of Maine: testing hypotheses of physical control using historical data. Marine Biology, 112: 165-174.

Garside, C., Garside, J.C., Keller, M.D., Sieracki, M.E., 1996. The formation of high nutrient low salinity water in the Gulf of Maine: A nutrient trap? Estuarine Coastal and Shelf Science, 42(5): 617-628.

Godin, G., 1968. The 1965 current survey of the Bay of Fundy: a new analysis of the data and interpretation of the results. 8, Marine Sciences Branch, Department of Mines and Technical Surveys.

Gribble, K.E., Keafer, B.A., Quilliam, M., Cembella, A.D., Kulis, D.M., Anderson, D.M., submitted. Distribution and toxicity of *Alexandrium ostenfeldii* (dinoflagellata) in the Gulf of Maine, USA. Deep Sea Research II.

He, R., McGillicuddy, D.J., Lynch, D.R., Smith, K.W., Stock, C.A., Manning, J.P., submitted. Data Assimilative Hindcast of the Gulf of Maine Coastal Circulation. Journal of Geophysical Research.

Hetland, R.D., McGillicuddy, D.J., Signell, R.P., 2002. Cross-frontal entrainment of plankton into a buoyant plume: the frog tongue mechanism. Journal of Marine Research, 60(6): 763-777.

Keafer, B.A., Anderson, D.M., 1993. Use of remotely-sensed sea surface temperatures in studies of *Alexandrium tamarense* bloom dynamics. In: T.J. Smayda and Y. Shimizu (Editors), Toxic phytoplankton blooms in the sea. Elsevier Science Publishers, pp. 763-768.

Keafer, B.A., Buesseler, K.O., Anderson, D.M., 1992. Burial of living dinoflagellate cysts in estuarine and nearshore sediments. Mar. Micropaleontol., 20: 147-161.

Keafer, B. A., Churchill, J. H., Anderson, D. A., submitted. Blooms of the toxic dinoflagellate, *Alexandrium fundyense* in the Casco Bay region of the western Gulf of Maine: advection from offshore source populations and interactions with the Kennebec River plume. Deep-Sea Research II.

Kirn, S. L., Townsend, D. W., Pettigrew, N. R., submitted. Suspended *Alexandrium* spp. Hypnozygote Cysts in the Gulf of Maine. Deep-Sea Research II.

Langdon, C., 1987. On the causes of interspecific differences in the growth-irradiance relationships for phytoplankton. Part I. A comparative study of the growth irradiance relationships of three marine phytoplankton species: *Skelotonema costatum, Olithodiscus luteus* and *Gonyaulax tamarensis*. Journal of Plankton Research, 9(3): 459-482.

Langdon, C., 1988. On the causes of interspecific differences in the growth-irradiance relationship for phytoplankton. Part II: A general review. Journal of Plankton Research, 10(6): 1291-1312.

Liebig, J., 1845. On chemical processes in the nutrition of vegetables, Chemistry and its applications to agriculture and physiology. L. Playfair, Peterson, PA.

Love, R. C., Loder, T. C., Keafer, B. A., submitted. Nutrient conditions during *Alexandrium fundyense* blooms in the western Gulf of Maine, USA. Deep Sea Research II.

Luerssen, R. M., Thomas, A. C., Hurst, J., submitted. Relationships between satellite-measured thermal features and *Alexandrium*-imposed toxicity in the Gulf of Maine. Deep Sea Research II.

Lynch, D.R., Hannah, C.G., 2001. Inverse Model for Limited-Area Hindcasts on the Continental Shelf. Journal of Atmospheric and Oceanic Technology, 18: 962-981.

Lynch, D.R., Holboke, M.J., Naimie, C.E., 1997. The Maine coastal current: spring climatological circulation. Continental Shelf Research, 17: 605-634.

Lynch, D.R., Ip, J.T.C., Naimie, C.E., Werner, F.E., 1996. Comprehensive coastal circulation model with application to the Gulf of Maine. Continental Shelf Research, 16: 875-906.

MacIntyre, J.G., Cullen, J.J., Cembella, A.D., 1997. Vertical migration, nutrition and toxicity in the dinoflagellate *Alexandrium tamarense*. Marine Ecology Progress Series, 148: 201-216.

Martin, J.L., White, A.A., 1988. Distribution and abundance of the toxic dinoflagellate *Gonyaulax excavata* in the Bay of Fundy. Can. J. Fish. Aquat. Sci., 45(11): 1968-1975.

Martin, J. L., Page, F. H., Hanke, A., Strain, P. M., LeGresley, M. M., submitted. *Alexandrium fundyense* Vertical Distribution Patterns during 1982, 2001 and 2002 in the offshore Bay of Fundy, Eastern Canada. Deep Sea Research II.

Matrai, P., Thompson, B., Keller, M., submitted. Circannual excystment of resting cysts of *Alexandrium* spp. from eastern Gulf of Maine populations. Deep-Sea Research II.

McGillicuddy, D.J., Signell, R.P., Stock, C.A., Keafer, B.A., Keller, M.D., Hetland, R.D., Anderson, D.M., 2003. A mechanism for offshore initiation of harmful algal blooms in the coastal Gulf of Maine. Journal of Plankton Research, 25(9): 1131-1138.

McGillicuddy, D. J., Anderson, D. M., Solow, A. R., Townsend, D. W., submitted. Interannual variability of *Alexandrium fundyense* abundance and shellfish toxicity in the Gulf of Maine. Deep-Sea Research II.

Naimie, C.E., 1996. Georges Bank residual circulation during weak and strong stratification periods: prognostic numerical model results. J. Geophys. Res., 101: 6469-6486.

Naimie, C.E., Limeburner, R., Hannah, C.G., Beardsley, R.C., 2001. On the geographic and seasonal patterns of the near-surface circulation on Georges Bank-- from real and simulated drifters. Deep-Sea Research II, 48: 501-518.

Page, F.H., Martin, J.L., Hanke, A., LeGresley, M., 2002. Temporal and spatial patterns in phytoplankton community structure within the Bay of Fundy, Xth International Conference on Harmful Algae, St. Petersburg, FL, USA.

Petrie, B., Yeats, P., 2000. Annual and interannual variability of nutrients and their estimated fluxes in the Scotian Shelf - Gulf of Maine region. Can. J. Fish. Aquat. Sci., 57: 2536-2546.

Pettigrew, N.R., Townsend D. W., Xue H., Wallinga J. P., Brickley P. J., Hetland R. D., 1998. Observations of the Eastern Maine Coastal Current and its offshore extensions in 1994. Journal of Geophysical Research, Vol. 103(C13): 30,623-30,639.

Platt, T., Jassby, A.D., 1976. The relationship between photosynthesis and light for natural assemblages of coastal marine phytoplankton. Journal of Phycology, 12: 421-430.

Poulton, Keafer, Kulis, Anderson, submitted. Toxin variability in natural populations of *Alexandrium fundyense* in Casco Bay, Maine - a potential indicator of nitrogen limitation. Deep Sea Research II.

Poulton, N.J., 2001. Physical and behavioral diagnostics of nitrogen limitation for the toxic dinoflagellate *Alexandrium fundyense*. PhD Thesis, Massachusetts Institute of Technology, Cambridge, Massachusetts, 246 pp.

Prakash, A., 1967. Growth and toxcity of a marine dinoflagellate, *Gonyaulax tamarensis*. Journal of the Fisheries Research Board of Canada, 24(7).

Shumway, S.E., Sherman-Caswell, S., Hurst, J.W., 1988. Paralytic shellfish poisoning in Maine: Monitoring a monster. Journal of Shellfish Research, 7(4): 643-652.

Signell, R.P., Jenter, H.L., Blumberg, A.F., 1993. Modeling the seasonal circulation in Massachusetts Bay, Estuarine and Coastal Modeling III, Oak Brook, Illinois, pp. 578-590.

Stock, C.A., McGillicuddy, D.J., Solow, A.R., Anderson, D.M., submitted. Evaluating hypotheses for the initiation and development of *Alexandrium fundyense* blooms in the western Gulf of Maine using a coupled physical-biological model. Deep Sea Research II.

Teegarden, G.J., Cembella, A.D., 1996. Grazing of toxic dinoflagellates, *Alexandrium* spp. by adult copepods of coastal Maine: implications for the fate of paralytic shellfish toxins in marine food webs. Journal of Experimental Marine Biology and Ecology, 196: 145-176.

Townsend, D.W., Bennett, S.L., Thomas, M.A., submitted-a. Diel and vertical distribution of *Alexandrium* spp. in the Gulf of Maine. Deep Sea Research II.

Townsend, D.W., Pettigrew, N.R., Thomas, A.C., 2001. Offshore blooms of the red tide dinoflagellate *Alexandrium* spp., in the Gulf of Maine. Continental Shelf Research, 21: 347-369.

Townsend, D.W., Pettigrew, N.R., Thomas, A.C., submitted-b. On the nature of offshore *Alexandrium fundyense* blooms in the Gulf of Maine. Deep Sea Research II.

Turner, J.T., Tester, P.A., 1997. Toxic marine phytoplankton, zooplankton grazers, and pelagic food webs. Limnology and Oceanography, 5(2): 1203-1214.

Turner, J. T., Borkman, D. G., submitted. Impact of zooplankton grazing on *Alexandrium* Blooms in the offshore Gulf of Maine. Deep Sea Research II.

Turpin, D.H., Dobel, P.E.R., Taylor, F.J.R., 1978. Sexuality and cyst formation in Pacific strains of the toxic dinoflagellate *Gonyaulax tamarensis*. Journal of Phycology, 14: 235-238.

Watras, C.J., Chisholm, S.W., Anderson, D.M., 1982. Regulation of growth in an estuarine clone of *Gonyaulax tamarensis* Lebour: salinity-dependent temperature responses. Journal of Experimental Marine Biology and Ecology, 62: 25-37.

White, A.W., Lewis, C.M., 1982. Resting cysts of the toxic red tide dinoflagellate *Gonyaulax excavata* in Bay of Fundy sediments. Can. J. Fish. Aquat. Sci., 39: 1185-1194.

Wyatt, T., Jenkinson, I.R., 1997. Notes on *Alexandrium* population dynamics. Journal of Plankton Research, 19(5): 551-575.

Xue, H.J., Chai, F., Pettigrew, N.R., 2000. A model study of the seasonal circulation in the Gulf of Maine. Journal of Physical Oceanography, 30(5): 1111-1135.

Yamamoto, T., Seike, T., Hashimoto, T., Tarutani, K., 2002. Modeling the population dynamics of the toxic dinoflagellate *Alexandrium tamarense* in Hiroshima Bay, Japan. Journal of Plankton Research, 24(1): 33-47.

Figure Captions

Figure 1. Schematic of the Maine Coastal Current. Branch points are located at (1) Penobscot Bay, (2) Cape Ann, and (3) Great South Channel. Seven segments of the current are indicated: (E)astern, (J)ordan, (W)estern, (M)assachusetts, (S)tellwagen, (N)antucket, and (G)eorges Bank. Figure redrafted from Lynch et al. (1997) with the addition of the Bay of Fundy gyre system as drawn in Godin (1968). Dashed white lines denote state boundaries of Maine (ME), New Hampshire (NH), and Massachusetts (MA).

Figure 2. A population dynamics model for *A. fundyense*. (a) Distribution of cysts (number of cysts cm^{-3}) in the upper 3cm of sediment derived from a 1997 survey of the Gulf of Maine (McGillicuddy et al., 2003) and surveys of the Bay of Fundy in 1981 (White and Lewis, 1982), 1982 and 1983 (data provided by Jennifer Martin, DFO). (b) Germination potential (decimal fraction of cysts able to germinate) as a function of time; the solid line is a piecewise linear fit to laboratory observations (open circles) of *A. fundyense*'s endogenous clock from Anderson and Keafer (1987). (c) Germination rate (% d^{-1}) as a function of temperature and light. Light has been converted to depth using a diffuse attenuation coefficient and the mean surface irradiance. Solid circles indicate laboratory germination experiments. (d) Specific growth rate (d^{-1}) as a function of temperature and salinity. Solid circles indicate growth rate measurements from laboratory cultures.

Figure 3. Distribution of *Alexandrium* spp. in the Gulf of Maine observed in June, July, and August of 1998 (from Townsend et al., 2001).

Figure 4. Climatological conditions for March-April (left column), May-June (middle column), and July-August (right column). Top two rows: observed temperature and salinity (available at http://www-nml.dartmouth.edu/). Third row: nitrate fields computed from temperature and salinity based on empirical relationships described in Garside et al. (1996). Nitrate values for salinities of less than 31.3 have been set to that of the nearest neighboring point with salinity greater than 31.3. Next three rows: growth rate as a function of irradiance, temperature, and salinity [$\mu(E,T,S)$], growth rate as a function of nitrate concentration, temperature, and salinity [$\mu(\mathrm{NO}_3,T,S)$], and overall growth rate [$\mu(E,\mathrm{NO}_3,T,S)=\min\left(\mu(E,T,S),\mu(\mathrm{NO}_3,T,S)\right)$]. Bottom row: specific rate of encystment [$En=\left(\mu\left(E,T,S\right)-\mu\left(\mathrm{NO}_3,T,S\right)\right)$ for $\mu(\mathrm{NO}_3,T,S)<\mu(E,T,S)$; $En=0$ elsewhere].

Figure 5. Simulated *A. fundyense* distribution for germination only (Run 1, left column), germination, growth and mortality (Run 2, middle column), and germination, growth, mortality and nutrient limitation (Run 3, right column). Mid-month snapshots of model output from May through August are shown in each row. The following bathymetric contours are overlayed: 60, 100, 150, 200, and 400 m.

Figure 6. Simulated *A. fundyense* distribution for an initial inoculum of 10 cells l^{-1} together with growth, mortality and nutrient limitation (Run 4). Mid-month snapshots of model output from May through August are shown in each panel. The following bathymetric contours are overlayed: 60, 100, 150, 200, and 400 m.

Figure 7. Cumulative distribution of new *A. fundyense* cysts diagnosed from Run 3. Mid-month snapshots of model output from May through August are shown in each panel. The following bathymetric contours are overlayed: 60, 100, 150, 200, and 400 m.

Figure 8. Conceptual model of the large-scale seasonal variations in *A. fundyense* vegetative cells and long-term maintenance of the two major cyst deposits in the Gulf of Maine.

Run	Initial Cell Concentration	Germination Input	Growth and Mortality	Nutrient Limitation	Run Identifier
1	C=0	yes	no	no	cell98_a6_new
2	C=0	yes	yes	no	cell98_a1_new
3	C=0	yes	yes	yes	cell98_a7_new_cor2
4	C=10	no	yes	yes	cell98_a8m

Table 1: Run table.

Symbol	Definition	Units	Value
K_N	Half-saturation constant for nutrient limited growth	μM	1.5
m	Mortality rate	d^{-1}	0.1
μ_{max}	Maximum growth rate	d^{-1}	0.6
μ_o^r	Basal respiration rate	d^{-1}	0.05
α_q	Growth efficiency	$d^{-1} W^{-1} m^2 s$	0.017
d_q	Germination depth	cm	1.0
E_{lgt}	Light level for germination under "light" conditions	$W m^{-2}$	2.4
E_{drk}	Light level for germination under "dark" conditions	$W m^{-2}$	0.024
k_w	Diffuse attenuation coefficient (water column)	m^{-1}	0.2
k_s	Diffuse attenuation coefficient (sediment)	mm^{-1}	3
E_0	Surface irradiance	$W m^{-2}$	280

Table 2. Parameters of the *A. fundyense* population dynamics model.

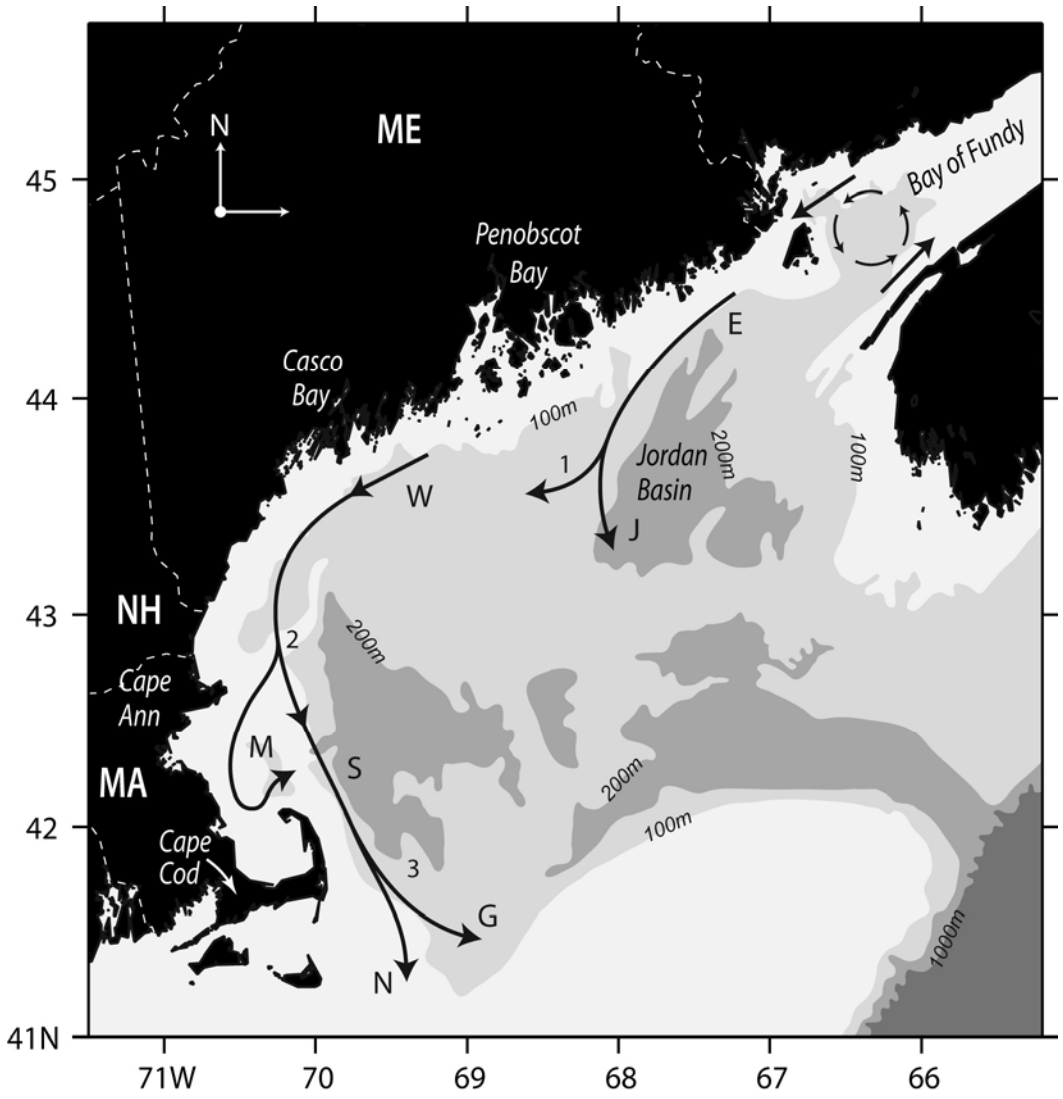
N
ME
Penobscot Bay
Bay of Fundy
Casco Bay
E
100m
1
W
Jordan Basin
200m
100m
J
NH
2
200m
Cape Ann
M
S
MA
200m
100m
Cape Cod
3
G
N
1000m
45
44
43
42
41N
71W
70
69
68
67
66

Figure 1

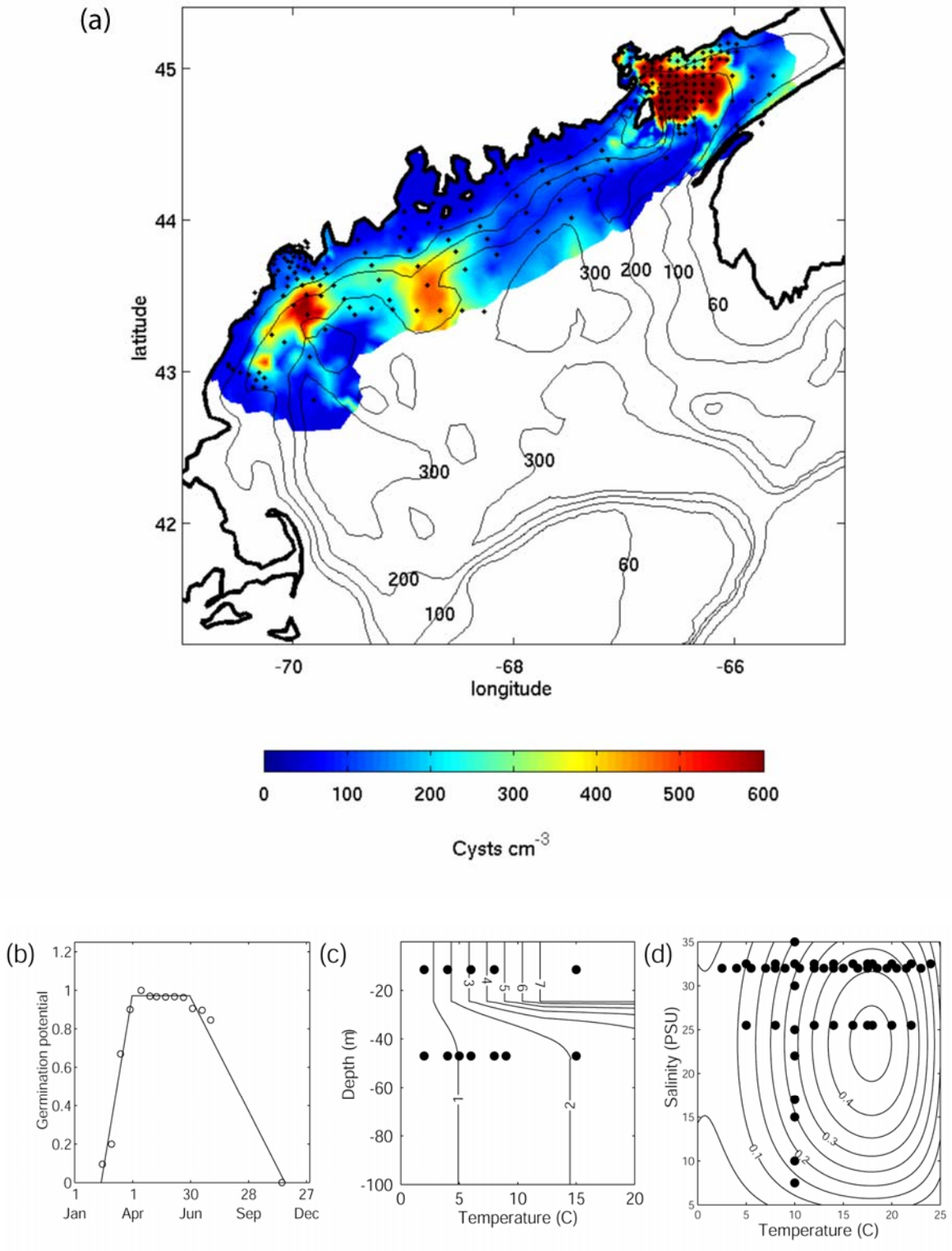
(a)
45
44
43
42
latitude
300
200
100
60
300
300
60
200
100
-70
-68
-66
longitude
0
100
200
300
400
500
600
Cysts cm-3
(b)
Germination potential
1.2
1
0.8
0.6
0.4
0.2
0
1
Jan
1
Apr
30
Jun
28
Sep
27
Dec
(c)
Depth (m)
-20
-40
-60
-80
-100
3
4
5
6
7
1
2
0
5
10
15
20
Temperature (C)
(d)
Salinity (PSU)
35
30
25
20
15
10
5
0.4
0.3
0.1
0.2
0
5
10
15
20
25
Temperature (C)

Figure 2

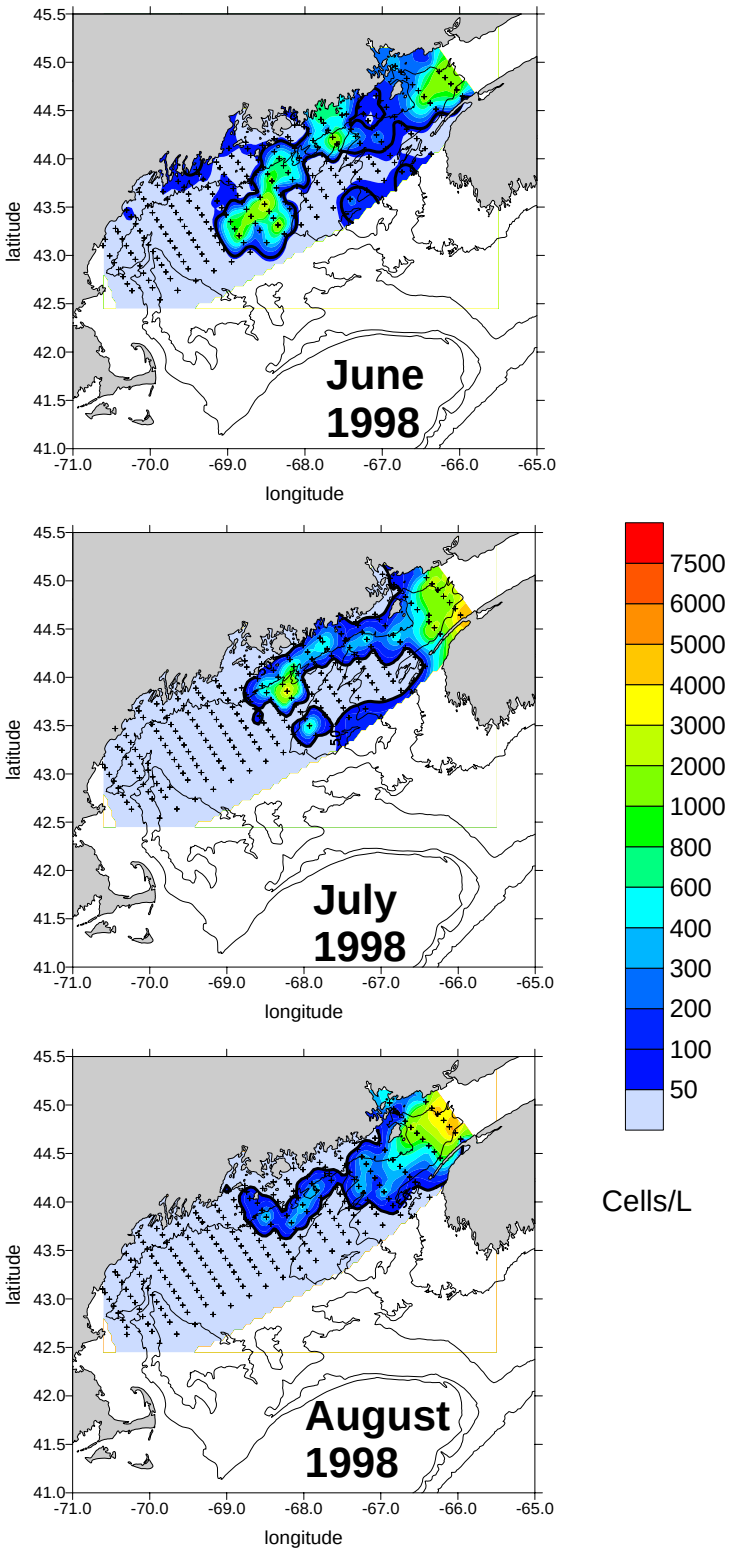
June
1998
July
1998
August
1998
latitude
longitude
45.5
45.0
44.5
44.0
43.5
43.0
42.5
42.0
41.5
41.0
-71.0
-70.0
-69.0
-68.0
-67.0
-66.0
-65.0
7500
6000
5000
4000
3000
2000
1000
800
600
400
300
200
100
50
Cells/L

Figure 3

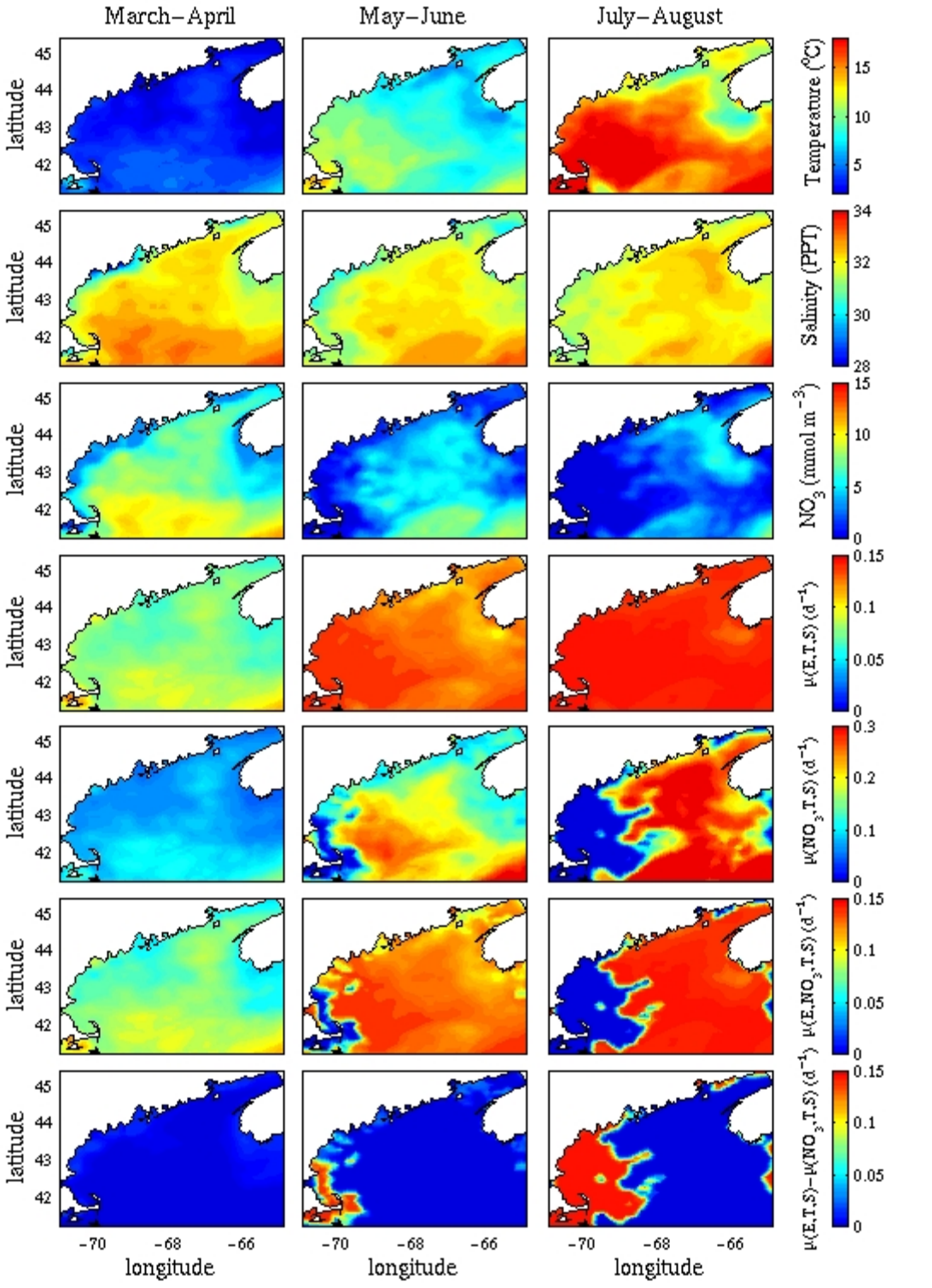
March–April
May–June
July–August
latitude
longitude
Temperature (°C)
Salinity (PPT)
NO3 (mmol m−3)
μ(E,T,S) (d−1)
μ(NO3,T,S) (d−1)
μ(E,NO3,T,S) (d−1)
μ(E,T,S)−μ(NO3,T,S) (d−1)
diag−blend−cor2m: 09−Dec−2004

Figure 4

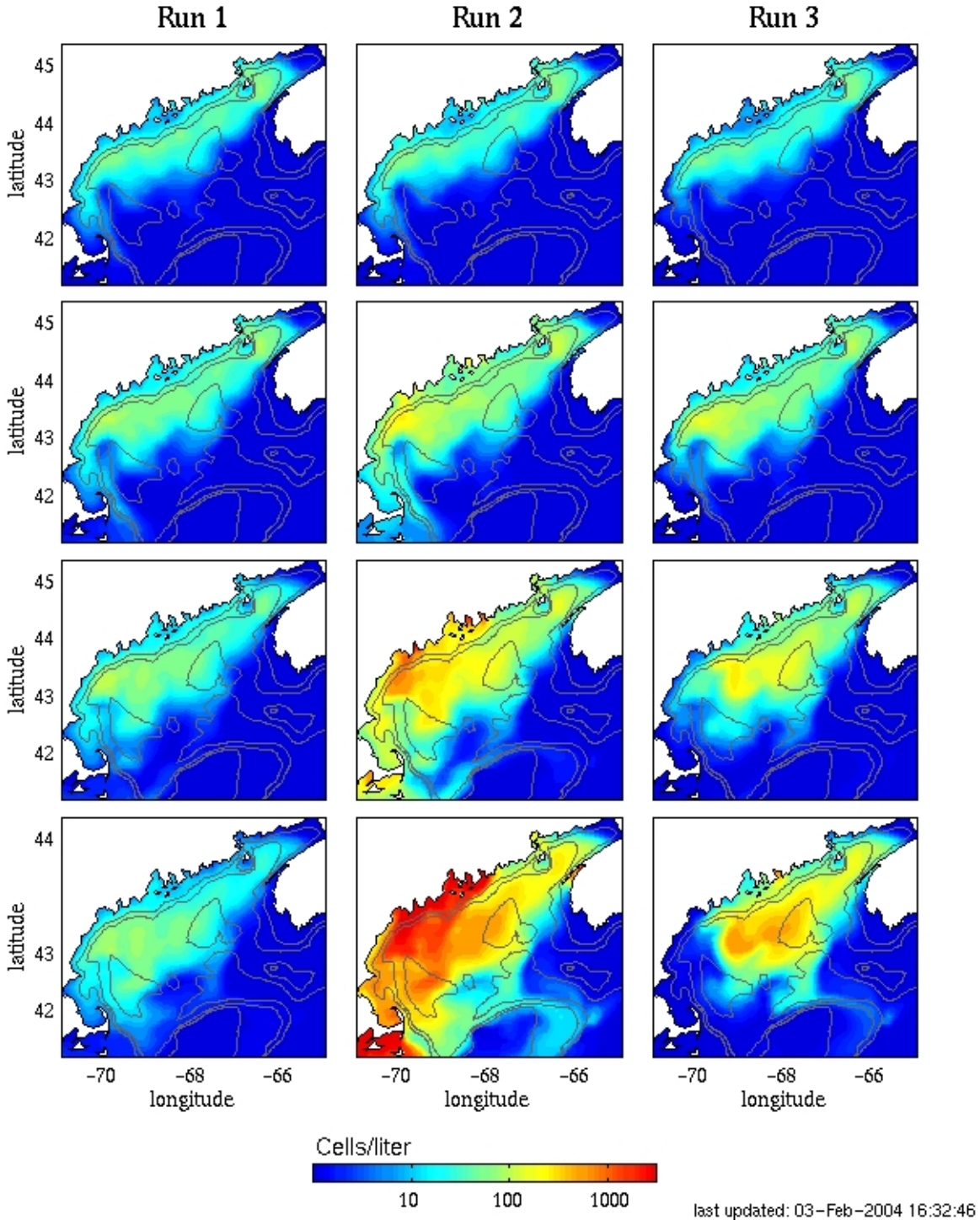
Run 1
Run 2
Run 3
latitude
longitude
45
44
43
42
-70
-68
-66
Cells/liter
10
100
1000
last updated: 03-Feb-2004 16:32:46

Figure 5

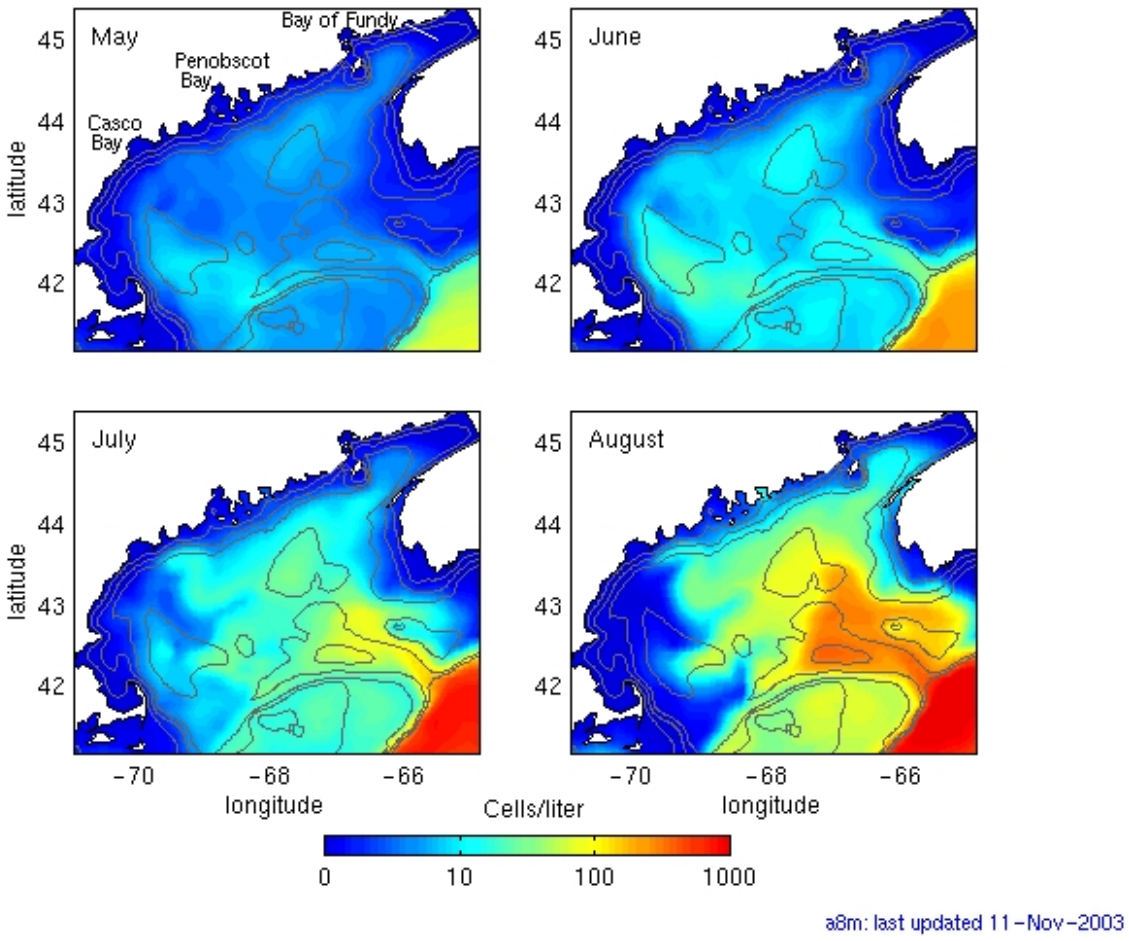
May
Bay of Fundy
Penobscot Bay
Casco Bay
June
July
August
45
44
43
42
latitude
-70
-68
-66
longitude
Cells/liter
0
10
100
1000
a8m: last updated 11-Nov-2003

Figure 6

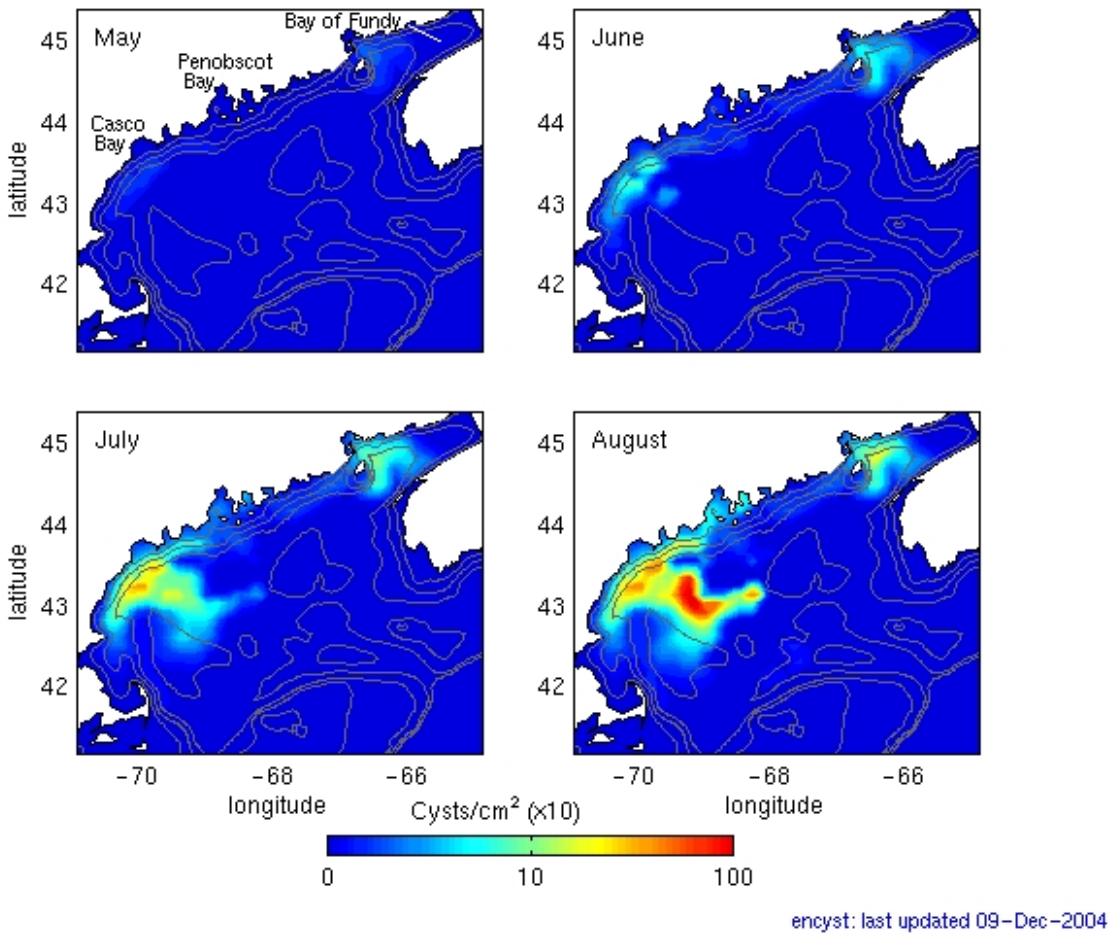
May
Bay of Fundy
Penobscot Bay
Casco Bay
June
July
August
45
44
43
42
latitude
-70
-68
-66
longitude
Cysts/cm^2 (x10)
0
10
100
encyst: last updated 09-Dec-2004

Figure 7

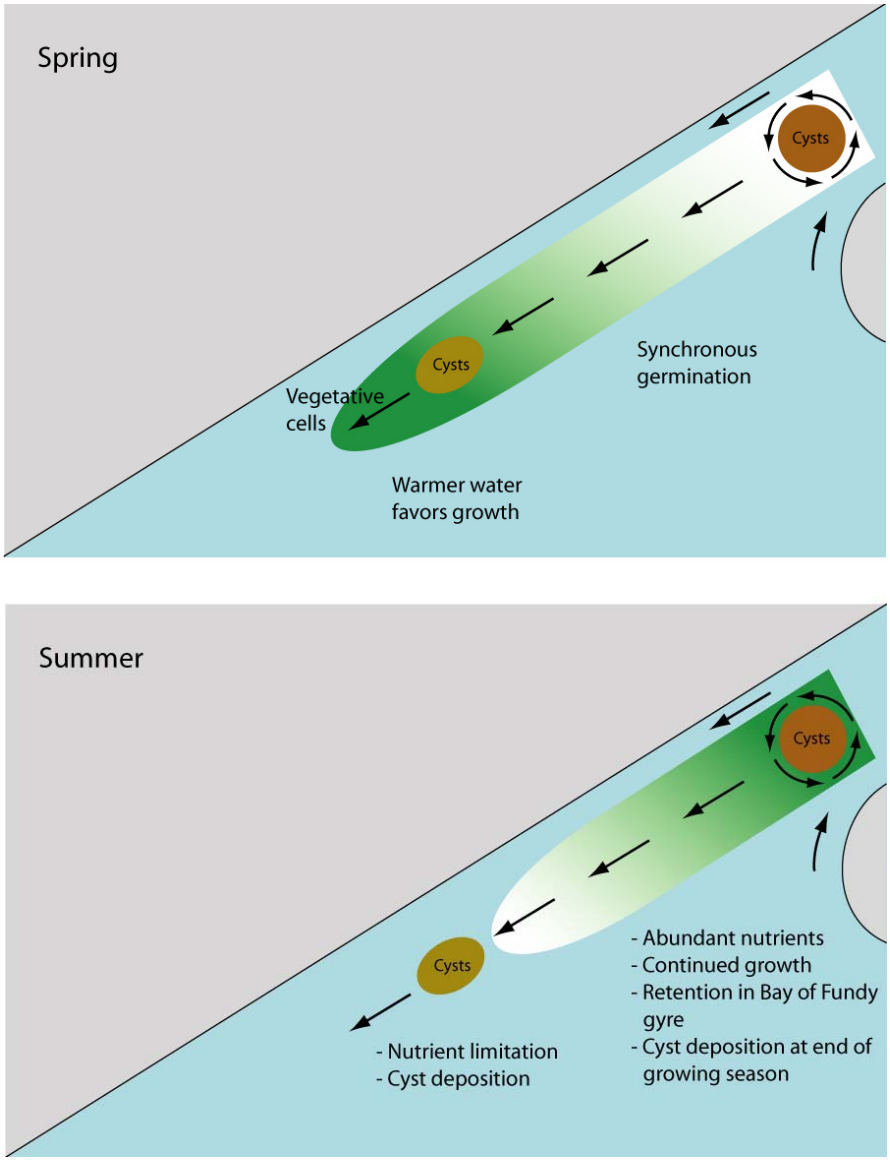
Spring
Cysts
Cysts
Vegetative cells
Synchronous germination
Warmer water favors growth
Summer
Cysts
Cysts
- Abundant nutrients
- Continued growth
- Retention in Bay of Fundy gyre
- Cyst deposition at end of growing season
- Nutrient limitation
- Cyst deposition

Figure 8